

Evaluating deep coal rock gas fracturing sweet spot intervals using PSO-ELM algorithm and petrophysical logging data

Received: 8 December 2025

Accepted: 21 May 2026

Published online: 27 May 2026

Cite this article as: Liu Z., Wang D., Yang B. *et al.* Evaluating deep coal rock gas fracturing sweet spot intervals using PSO-ELM algorithm and petrophysical logging data. *Sci Rep* (2026). <https://doi.org/10.1038/s41598-026-54924-z>

ZhiDi Liu, Duo Wang, Binrui Yang, Jidong Tang, Chengwang Wang, Wei Wang, Xinsi Hu & Jingnan Zhang

We are providing an unedited version of this manuscript to give early access to its findings. Before final publication, the manuscript will undergo further editing. Please note there may be errors present which affect the content, and all legal disclaimers apply.

If this paper is publishing under a Transparent Peer Review model then Peer Review reports will publish with the final article.

© The Author(s) 2026. **Open Access** This article is licensed under a Creative Commons Attribution-NonCommercial-NoDerivatives 4.0 International License, which permits any non-commercial use, sharing, distribution and reproduction in any medium or format, as long as you give appropriate credit to the original author(s) and the source, provide a link to the Creative Commons licence, and indicate if you modified the licensed material. You do not have permission under this licence to share adapted material derived from this article or parts of it. The images or other third party material in this article are included in the article's Creative Commons licence, unless indicated otherwise in a credit line to the material. If material is not included in the article's Creative Commons licence and your intended use is not permitted by statutory regulation or exceeds the permitted use, you will need to obtain permission directly from the copyright holder. To view a copy of this licence, visit <http://creativecommons.org/licenses/by-nc-nd/4.0/>.

Evaluating Deep coal rock gas fracturing sweet spot intervals using PSO-ELM algorithm and petrophysical logging data

ZhiDi Liu ^{1,2*}, Duo Wang ^{3*}, Binrui Yang ¹, Jidong Tang ¹, Chengwang Wang ⁴, Wei Wang ⁵, Xinsi Hu ¹, Jingnan Zhang ¹

1 School of Earth Science and Engineering, Xi'an shiyu university, Xi'an, Shaanxi 710065, China

2 Key Laboratory of Oil and Gas Reservoir Geology, Shaanxi Province, Xi'an 710065, China

3 Hancheng Gas Production Management Area of PetroChina Coal rock gas Co., Ltd., Xi'an, Shaanxi 710082, China

4 Linfen Gas Production Management Area of PetroChina Coal rock gas Co., Ltd., Taiyuan, Shanxi 030000, China

5 Exploration and Development Construction Branch of PetroChina Coal rock gas Co., Ltd., Xi'an, Shaanxi 710082, China

Abstract: The Daning Jixian block is situated on the eastern periphery of the Ordos Basin. it faces multiple challenges including strong reservoir heterogeneity and unclear identification of fracturing sweet spot interval intervals, which restrict the enhance productivity and operational efficiency of deep coal rock gas. This study adopts an integrated geology-engineering approach and employs ensemble optimized machine learning algorithms to predict fracturing sweet spot interval intervals. The recent exploration and development experiences along with extensive geological and production data in the block are summarized, 10 key controlling factors for reservoir quality and engineering quality are selected and organized into a dataset. The PSO-ELM algorithm was programmed on the MATLAB platform, into which this dataset was imported for iterative prediction. This process established a graded evaluation model for fracturing sweet spot interval interval intervals based on the PSO-ELM algorithm. The model was applied to predict the fracturing sweet spot intervals in the No. 5 and No. 8 coal seams of Well X-11, the overall prediction accuracy exceeds 85%, with Class I sweet spot intervals being predominant. Spatial distribution analysis across the block revealed abundant Class I and II sweet spots, confirming substantial exploitable high-quality resources. These predictions were validated by subsequent perforation and fracturing operation data, demonstrating that this methodology provides reliable logging technology support for perforation interval selection and fracturing stimulation optimization in deep coal reservoir development.

Keywords: Deep coal rock gas; Geological engineering integration; PSO-ELM algorithm; Main controlling factors; Fracturing sweet-spot intervals

*Corresponding author (Communication with the editorial department): ZhiDi Liu. E-mail: liuzhidi@xsyu.edu.cn

*Corresponding author: Duo Wang. E-mail: 1218808185@qq.com

1 Introduction

The development of coal rock gas in the mid-shallow strata of the eastern Ordos Basin has achieved initial scale, with the Daning-Jixian Block emerging as China's first large, integrated coal rock gas field with a burial depth exceeding 2000 m, proven reserves surpassing $762 \times 10^8 \text{ m}^3$, and high resource abundance. It has become a key area for the exploration and development of deep coal rock gas (Wang et al., 2024). Initially focused on tight gas exploration in the Permian Shihezi Formation, the block's exploration focus has gradually shifted towards coal rock gas in the Carboniferous Taiyuan and Benxi Formations, as the quality of tight gas resources has declined. The

First author and corresponding author: ZhiDi Liu (1978-), male, PhD, professor, specializing in logging evaluation for unconventional reservoir, etc. E-mail: liuzhidi@xsyu.edu.cn.

Second corresponding author: Duo Wang (1996-), male, doctoral student, specializing in rock mechanics and unconventional reservoir logging evaluation, as well as integrated geological engineering evaluation of coal rock gas. E-mail: 1218808185@qq.com.

Taiyuan and Benxi Formations exhibit superior coal-forming environments, featuring vertically distributed No. 5 and No. 8 coal seams with burial depths greater than 1500 m. These formations are characterized by relatively simple structures, underdeveloped faults, favorable coal body structures, significant effective thickness, and generally high gas content, falling within the realm of deep coal rock gas and holding substantial resources and great exploration potential.

Numerous scholars worldwide have conducted fruitful research on this subject, yielding a wealth of valuable insights and practical achievements. These issues severely constrain the efficient and comprehensive development of deep coal rock gas in this region. Analysis of geological data from the No. 5 and No. 8 coal seams in the Daning-Jixian Block, based on the quantitative evaluation of fractability using elastic parameters and stress characteristics, indicates that better gas production results are achieved when the fractability index exceeds 0.6 (Wang et al., 2022). The enrichment of coal rock gas is influenced by factors such as the lithology of the roof and floor, geological structure, and coal characteristics, with the depositional environment primarily affecting the lithological combination and sealing characteristics of the roof and floor (Wang et al., 2024; Li et al., 2022). Effective coal seam thickness, structure, and hydrodynamic conditions significantly impact enrichment, while abundance, gas content, and a comprehensive fractability index are key criteria for evaluating favorable geology-engineering areas (Zheng et al., 2024). Saturation can be estimated using the Langmuir equation and methane adsorption isotherms, and combining this with effective coal seam thickness and gas content helps determine optimal well placement (Banerjee et al., 2021). Core indicators for evaluating sweet spots in deep coal rock gas include resource potential (coal reservoir energy) and fractability (structure, vertical fracture zones, stress difference between roof/floor and coal seam). This necessitates developing new methods that integrate fractal theory for quantification and numerical simulation to characterize fracture complexity (Liu et al., 2023). The enrichment model for deep coal rock gas is described as "fold-fault-hydrodynamic," with enrichment zones located in structurally gentle areas and slope zones. Establishing a highly efficient development technology system for deep coal rock gas under the framework of geology-engineering integration is crucial (Xu et al., 2024; Guo et al., 2024). Three-dimensional geological modeling enables detailed characterization of deep coal measures and quantitative representation of reservoir heterogeneity (Zhang, 2013).

Techniques such as frequency division attribute inversion and spectral imaging can predict coal seam thickness and gas content. Developing 3D static reservoir property models helps analyze spatial distribution, and the Analytic Hierarchy Process (AHP) based on fuzzy mathematics can establish optimal sweet spot evaluation models (Wang et al., 2016; Mondal et al., 2024). Conventional seismic techniques, integrating borehole data with seismic profiles, can identify faults and fractures, facilitating the division of coal rock gas sweet spots (Urosevic et al., 2000). Subtle structural variations significantly control high production in deep coal rock gas wells. Methodologies based on "geology-engineering" sweet spot coefficients, the "Black Gold" target concept, and classification standards, allow for building "geology-engineering" sweet spot models along horizontal wells (Yan et al., 2021; Xu et al., 2024). Multi-parameter weighted stepwise evaluation methods based on inversion yield sweet spot distributions that better align with

geological principles (Wei et al., 2023). Studying the gas desorption potential using the desorption index and hydrodynamics using drawdown parameters, coupled with fuzzy AHP, aids in development sweet spot prediction (Fu et al., 2021). Pre-stack inversion to obtain fluid-indicative attributes and analyzing AVO characteristics using pseudo-linear Zoeppritz equations have proven effective for predicting sweet spots (Dong et al., 2018).

The development of deep coal rock gas currently faces several major challenges, including strong reservoir heterogeneity, unclear primary controls on enrichment, and difficulties in identifying optimal fracturing intervals (Lin, 2019). The failure to place perforations within high-quality sweet spots during stage selection has led to low productivity in some individual wells, emerging as a critical bottleneck for production enhancement. With the deepening of exploration and development practices and the evolution of theoretical research, a true fracturing sweet spot is now understood as an area characterized by suitable coal seam thickness, moderate thermal maturity, favorable gas content, good porosity and permeability, low stress contrast, and high fractability. This concept extends the traditional reservoir sweet spot to include engineering attributes. However, a reservoir sweet spot alone may be technically unfracturable, while an engineering sweet spot alone may lack reservoir production potential. This disconnect creates significant contradictions when applying geological or engineering sweet spots to guide field operations, particularly reservoir stimulation. The root cause lies in the separate prediction of reservoir and engineering sweet spots without adequately addressing their intrinsic coupling relationship (Sang et al., 2023), resulting in a lack of integration mechanism and organic unity between geological and engineering sweet spots. To address these limitations of traditional evaluation methods, this study, guided by the philosophy of geology-engineering integration and leveraging machine learning techniques, aims to achieve organic fusion of reservoir and engineering sweet spots through multi-parameter data analysis. This approach is designed to enable accurate and effective evaluation of geology-engineering sweet spot intervals in the deep coal reservoirs of the Daning-Jixian Block, thereby providing crucial logging technology support for optimizing perforation intervals and enhancing fracture stimulation in deep coal rock gas development.

2 Geological settings

The Daning-Jixian Block is located on the southeastern margin of the Ordos Basin. Structurally, it lies within the western slope zone of the Jinxi Fold Belt, at the eastern end of the Weibei Uplift and the eastern part of the Yimeng Uplift. The overall structure is a west-dipping monocline (Figure 1), exhibiting a fundamental tectonic framework described as "one uplift, one depression, and two slopes" with distributed faults. This framework comprises the central Taoyuan Anticline Belt, the Puxian Depression Belt, the eastern Mingzhu Slope Belt, and the western slope belt, trending approximately 30°. The overall structure is relatively simple, with formation dips less than 1° and no significant structural undulations (Li et al., 2024). The Upper Paleozoic strata are continuously developed from top to bottom, including the Upper Permian Shiqianfeng Formation, the Middle Permian Upper and Lower Shihezi Formations, the Lower Permian Taiyuan and Shanxi Formations,

and the Upper Carboniferous Benxi Formation (Figure 2). The total sedimentary thickness ranges from 650- 900 m, with an average of 800 m (Yang et al., 2004; Allegra et al., 2022).

The current primary target for deep coal-measure gas exploration and development is the Benxi Formation. This formation represents a coastal to shallow marine sedimentary sequence. Controlled by the depositional environment, it belongs to a transitional facies from a delta front subfacies to a lagoon-tidal flat subfacies. The upper part is primarily composed of light grey aluminous mudstone, while the lower part mainly consists of interbedded sandy conglomerate and sandy mudstone. The base often contains honeycomb-like limonite, exhibiting a parallel unconformity contact with the underlying strata, the formation thickness varies from 9-35 m, averaging 15m.

A widely distributed, basin-wide stable coal seam, the No. 8 coal seam, is developed in the upper part of the Benxi Formation. The coal-forming precursor was low herbaceous plants. This seam is characterized by a high degree of coalification, significant thickness, high gas content, well-developed cleats and fractures, and is predominantly composed of primary structure coal. The No. 8 seam has a burial depth of 2200-2400 m, a thickness of 5-12 m, a high thermal maturity, and a dip angle of 0.34°-0.46°. Faults are undeveloped. The maceral composition is mainly bright and semi-dull coal (Peng et al., 2024). The vitrinite content is 62.02%, inertinite 19.41%, and mineral matter 18.57%. The mean random vitrinite reflectance (Ro) is 2.47%. The gas content ranges from 20 to 35 m³/t, and the average reservoir pressure is 20 MPa. Overall, the conditions for deep coal-measure gas development in this area are favorable.

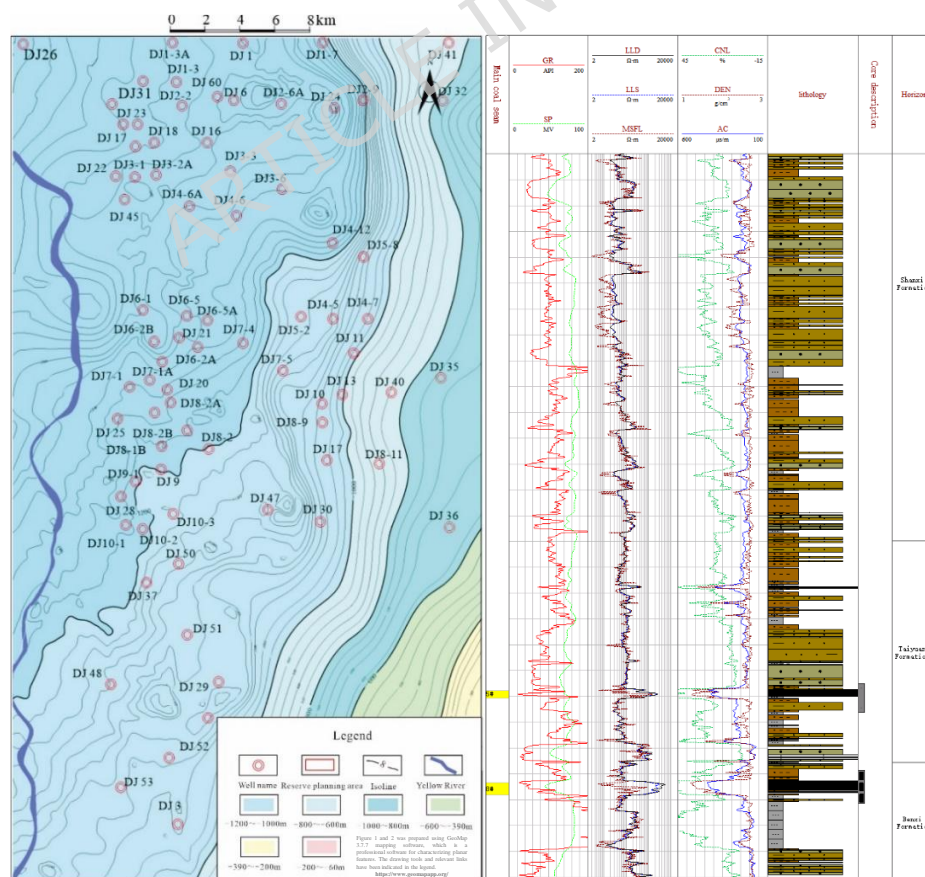


Figure caption: Figure 1 and 2 was prepared using GeoMap 3.7.7 mapping software, which is a professional software for characterizing planar features. The drawing tools and relevant links have been indicated in the legend.

Figure 1. Schematic diagram of the structural location of the Research Area (Left)

Figure 2. Comprehensive stratigraphic column chart of the Research Area (Right)

3 Theoretical basis

The enrichment degree of coal rock gas resources in deep coal reservoirs is governed by multifactorial interactions, which ultimately dictate the overall development efficiency of coal rock gas projects. In deep geological settings, key challenges for geological sweet-spot prediction include understanding:

Depth-dependent variations in rock mechanical parameters (e.g., strength, elasticity) and critical formation conditions (e.g., in-situ stress, temperature, pressure) under high-temperature and high-pressure (HTHP) environments; Multiphase methane occurrence mechanisms and dynamic transformation processes under deep in-situ geological conditions; Reservoir-forming response mechanisms and enrichment models under the coupling effects of sedimentation, tectonics, hydrodynamics, and other factors (Xia et al., 2017).

For engineering sweet-spot prediction, the challenge lies in the complex rock mechanical properties that hinder the formation of hydraulic fracture networks. However, the well-preserved primary coal structures and developed cleat-fracture systems in deep coal reservoirs provide favorable geological conditions for perforation and fracturing. Large-scale volume fracturing remains pivotal for achieving high-efficiency development of deep coal rock gas.

The factors influencing the gas production performance of deep coal rock gas reservoirs encompass both reservoir characteristics and engineering parameters. Reservoir sweet-spot prediction aims to identify zones of coal rock gas enrichment, with evaluation criteria focusing on reservoir properties such as petrophysical quality (e.g., porosity, permeability), gas-bearing capacity (e.g., gas saturation), fracture development intensity, and heterogeneity. Engineering sweet-spot prediction, meanwhile, targets intervals suitable for fracturing and perforation, evaluated through engineering parameters including rock mechanical properties (e.g., brittleness index) and stress contrast characteristics (e.g., horizontal stress difference coefficient). Based on extensive geological and operational data from the Research Area, ten key controlling factors (evaluation metrics) have been identified, closely linked to reservoir quality and engineering quality:

- Reservoir Quality (5 factors):
 - Carbon-to-ash ratio;
 - Porosity;
 - Permeability;
 - Gas saturation;
 - Fracture development index.
- Engineering Quality (5 factors):
 - Coal structure;
 - Brittleness index;
 - Fracture pressure;

Lateral pressure coefficient;
Horizontal stress difference coefficient.

3.1 Reservoir quality evaluation parameters

(1) Carbon to plaster ratio R_{fv}

The carbon to ash-mud ratio refers to the ratio of fixed carbon content to the sum of ash and shale content. This parameter holds significant importance in characterizing the quality evaluation of deep coalbed reservoirs. Fixed carbon represents the residual portion of coal after removing moisture, volatile matter, and ash. It primarily consists of carbon and directly reflects coal's combustion performance and calorific capacity, serving as a direct parameter for evaluating coalbed quality. Ash refers to the solid residue remaining after coal is completely burned under specified conditions. It originates from minerals in coal, such as clay, quartz, and pyrite. Higher ash content indicates poorer coalbed quality. Shale content denotes the proportion of extremely fine-grained clay mineral particles in coal, which affects its physical and chemical properties. Higher shale content also correlates with poorer coalbed quality. Therefore, the carbon to ash-mud ratio is a critical parameter reflecting the permeability, stability, and gas-bearing capacity of deep coal reservoirs. A higher ratio indicates better reservoir quality, and its calculation formula is:

$$R_{fv} = \frac{FC}{VASH + VSH} \quad (1)$$

where: R_{fv} is the carbon to ash-mud ratio, dimensionless; FC denotes the fixed carbon content, %; $VASH$ is the ash content, %; VSH is the mud content, %.

(2) Porosity φ

Porosity denotes the ratio of pore volume within deep coal reservoirs to the overall volume of the coal reservoir. (Cheng et al, 2021). It has various genesis types and sizes, and is the main site for coal rock gas accumulation and an important channel for diffusion seepage flow. The significance of porosity in characterizing reservoir quality mainly lies in three aspects: storage capacity, gas migration, and resource assessment. The larger the porosity, the more coal rock gas fluids can be stored in the coal reservoir; a higher porosity provides a wider flow space for gases, which facilitates their diffusion and permeation; reservoirs with high porosity are often considered to have greater resource potential. Therefore, increased porosity correlates with enhanced reservoir quality. (Lin,2019). The porosity of coal reservoirs is determined using the average of the cube roots of three porosity logs, and its calculation formula is as follows:

$$\varphi_{\Delta t} = \left[\frac{\Delta t - \Delta t_{ma}}{(\Delta t_f - \Delta t_{ma}) \times C_p} \right] - \left(\frac{V_{sh} \times (\Delta t_{sh} - \Delta t_{ma})}{\Delta t_f - \Delta t_{ma}} \right) \quad (2)$$

$$\varphi_{\rho_b} = \left[\frac{\rho_b - \rho_{ma}}{\rho_f - \rho_{ma}} \right] - \frac{V_{sh} \times (\rho_{sh} - \rho_{ma})}{\rho_f - \rho_{ma}} \quad (3)$$

$$\varphi_{CNL} = \varphi_N - V_{sh} \times \varphi_{Nsh} \quad (4)$$

$$\varphi = \frac{\varphi_{\Delta t} + \varphi_{\rho_b} + \varphi_{CNL}}{3} \quad (5)$$

where: $\varphi_{\Delta t}$ is the acoustic porosity,%; Δt is the acoustic travel time, $\mu\text{s}/\text{ft}$; Δt_{ma} is the acoustic travel time of the coal matrix, $\mu\text{s}/\text{ft}$; Δt_f is the acoustic travel time of the pore fluid, $\mu\text{s}/\text{ft}$; C_p is the compaction correction coefficient of the formation, dimensionless; V_{sh} is the shale content, %; Δt_{sh} is the acoustic travel time of shale, $\mu\text{s}/\text{ft}$; φ_{ρ_b} is the density porosity,%; ρ_b is the density, g/cm^3 ; ρ_{ma} is the density of the coal matrix, g/cm^3 ; ρ_f is the density of the pore fluid, g/cm^3 ; ρ_{sh} is the density of shale, g/cm^3 ; φ_{CNL} is the compensated neutron porosity of shale, %; φ_N is the compensated neutron porosity, %; φ_{Nsh} is the compensated neutron porosity of shale, %; φ is the porosity, %.

(3) Permeability K

Permeability refers to the ability of fluids to flow through pores and fractures in deep coal reservoirs under a certain pressure differential, indicating how easily fluids can move through the reservoir. Its significance in characterizing reservoir quality lies primarily in two aspects: fluid flow capacity and gas production efficiency. Reservoirs with higher permeability allow coal rock gas to flow more rapidly and smoothly into wellbores, thereby enhancing gas production efficiency and output. In practical extraction operations, areas with high permeability are often prioritized as "sweet spots" of high-quality reservoirs.

Table 1 Laboratory coring physical property test data of fractured coal rock and matrix coal rock

Fracture-developed coal rock coring test		Matrix coal rock coring test	
φ / (%)	K / (mD)	φ / (%)	K / (mD)
0.607	0.054	0.200	0.002
2.004	0.072	1.114	0.006
2.827	1.342	2.784	0.008
3.986	0.497	2.561	0.018
4.554	0.436	3.207	0.026
6.101	1.650	3.742	0.034
7.108	0.559	3.987	0.051
7.340	25.195	4.365	0.036
7.711	25.780	4.677	0.018
8.562	29.498	5.078	0.023
/	/	6.526	0.025
/	/	6.904	0.026
/	/	7.216	0.026
/	/	7.416	0.031
/	/	6.771	0.089
/	/	6.993	0.084
/	/	7.305	0.090
/	/	0.200	0.002

The porosity of coal seams directly affects permeability. Based on confining pressure porosity-permeability experimental data from core wells in the deep No. 8 coal seam (table 1), crossplots of porosity versus permeability were established to analyze their correlation. As shown in figures 3, permeability exhibits strong correlations with porosity in both fracture and matrix media. The calculation formula is:

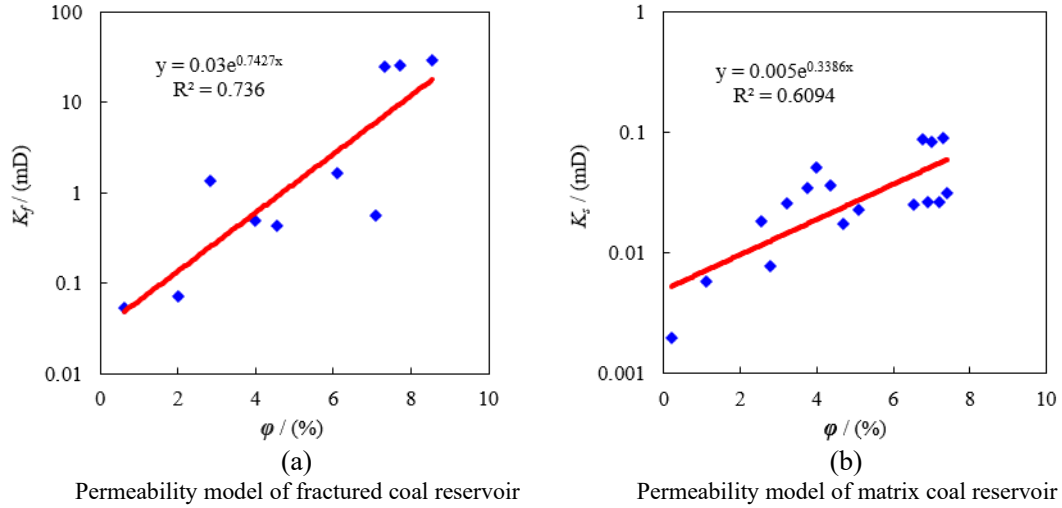


Figure 3. Two permeability modeling charts for coal reservoirs

$$\begin{cases} K_f = 0.03e^{0.7427\phi} \\ K_s = 0.005e^{0.3386\phi} \end{cases} \quad (6)$$

where: K_f is the fracture permeability, mD; K_s is the matrix permeability, mD; The meaning of other parameters is the same as above.

(4) Gas saturation S_g

The methane adsorption capability of coal seams is contingent upon temperature and pressure. At constant temperature, the adsorption amount increases with rising pressure. When reaching sufficiently high pressure, the coal's adsorption capacity becomes saturated, and further pressure increases no longer enhance adsorption. This adsorption characteristic conforms to the Langmuir equation. Gas saturation is defined as the ratio of the actual gas content to the theoretical gas content (Liu, 2024). Thus, the expression is as follows:

$$S_g = \frac{V_{ac}(P + P_L)}{V_L P} \quad (7)$$

where: V_{ac} represents the actual gas content of the coal seam, m^3/t ; V_L denotes the maximum adsorbed gas quantity at saturation(Langmuir volume), also known as m^3 ; P_L indicates the pressure at half-saturation adsorption(Langmuir pressure), MPa; P is the pore pressure, MPa.

Dr. Liu Zhi's research revealed significant correlations between fixed carbon and Langmuir volume, as well as between Langmuir volume and Langmuir pressure. Based on saturation test results and industrial component analysis from core samples of the deep No. 8 coal seam, linear cross-plots of fixed carbon versus Langmuir volume and Langmuir volume versus Langmuir pressure were established, as shown in figure 4 (a, b). This enables the prediction of gas saturation in the deep No. 8 coal seam of this block using the Langmuir equation. The calculation formulas for Langmuir volume and pressure are as follows:

$$\begin{cases} V_L = 11.294e^{0.0122FC} \\ P_L = 422.51V_L^{-1.5094} \end{cases} \quad (8)$$

where: The meaning of other parameters is the same as above.

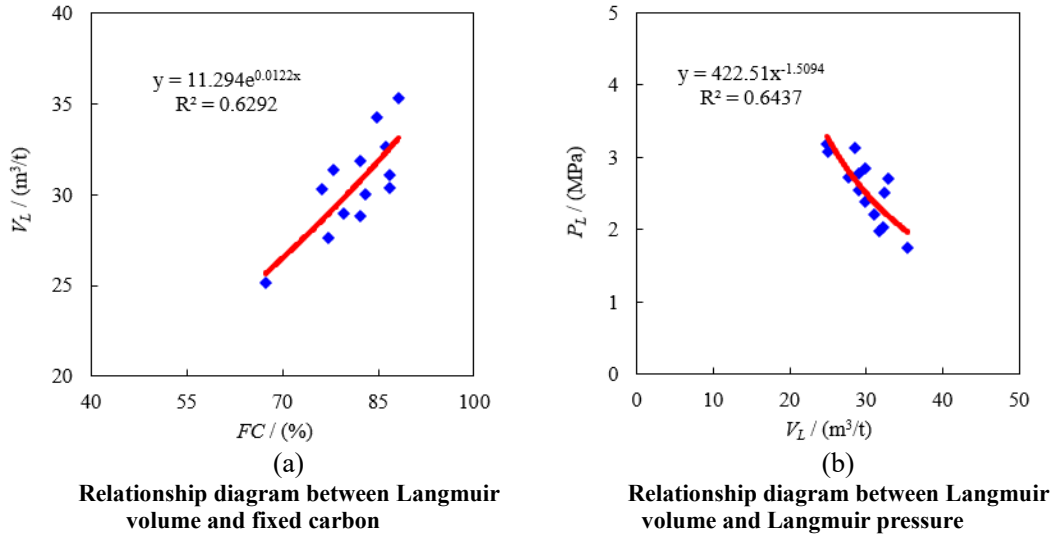


Figure 4. Determination plots for Langmuir volume and Langmuir pressure.

(5) Index of fracture development degree K_v

The fracture development degree index represents the squared ratio of the compressional wave velocity in coal seams to that in the intact coal matrix. When the compressional wave velocity in coal seams nears the matrix value (V. Vishal, 2013), the fracture development degree index increases, indicating less developed fractures; conversely, it suggests more developed fractures. The calculation formula is:

$$K_v = \left(\frac{V_p}{V_{pma}} \right)^2 \quad (9)$$

where: K_v is the fracture development degree index, dimensionless; V_p is the compressional wave velocity of coal rock, which can be replaced by the compressional wave velocity provided by logging data, m/s; V_{pma} is the compressional wave velocity of the coal rock matrix, m/s.

3.2 Engineering quality evaluation parameters

(1) Coal texture I_{cs}

Coal texture refers to the rock composition and internal structural characteristics of coal, mainly reflecting the influence of various geological processes experienced by coal in geological history. The original structure coal has good mechanical stability and can withstand large geostress without significant deformation and damage. Fragmented coal can still maintain a certain degree of stability, but is prone to further fragmentation when subjected to external disturbances. The mechanical stability of fragmented coal and mylonitic coal is extremely poor, and the fracturing production effect is extremely poor; the adsorption capacity of primary structured coal is strong (Tang et al, 2023), while the adsorption capacity of fragmented and mylonitic structured coal is greatly reduced due to the destruction of pore and fracture systems. Geophysical logging information has a strong ability to distinguish coal texture, and wellbore diameter, resistivity, density, and acoustic waves are sensitive to coal texture response. The calculation formula is:

$$I_{cs} = \frac{\rho_b}{\Delta t} \cdot \log \left(\frac{RT}{CAL} \right) \quad (10)$$

where: RT is the undisturbed coal seam resistivity, $\Omega \cdot m$; CAL is the wellbore diameter, in; The meaning of other parameters is the same as above.

(2) Brittleness index BI

The brittleness index of a coal seam characterizes the difficulty of hydraulic fracturing stimulation and serves as one of the key parameters for sweet spot evaluation in coal rock gas engineering. Generally, a higher brittleness index indicates easier formation of complex network fractures, whereas formations with lower brittleness indices tend to develop simple bi-wing fractures. The brittleness index can be characterized by the combined use of Young's modulus and Poisson's ratio. Poisson's ratio indicates the rock's resistance to failure under stress, with higher values corresponding to greater difficulty in fracture initiation. Young's modulus represents a rock's ability to maintain fractures after rupture, with higher values favoring the formation of complex fractures. The calculation formula is:

$$BI(\%) = \frac{\Delta E + \Delta PR}{2} \quad (11)$$

The standard values of Poisson's ratio and Young's modulus can be calculated using Equation (12).

$$\begin{cases} \Delta E = \frac{(E - E_{\min})}{E - E_{\min}} \times 100 \\ \Delta PR = \frac{(PR_{\max} - PR)}{PR_{\max} - PR_{\min}} \times 100 \end{cases} \quad (12)$$

where: BI is the coal seam brittleness index, %; ΔE is the standardized Young's modulus, dimensionless; ΔPR is the standardized Poisson's ratio, dimensionless; E is the Young's modulus of the coal seam, MPa; E_{\max} is the maximum Young's modulus values of coal seam, in MPa; E_{\min} is the minimum Young's modulus values of coal seam, in MPa; PR_{\max} is the maximum Poisson's ratio values of coal seam, dimensionless. PR_{\min} is the minimum Poisson's ratio values of coal seam, dimensionless.

(3) Horizontal stress difference coefficient P_{sd}

The horizontal stress difference coefficient is the ratio of differential horizontal in-situ stresses to the minimum primary stress, characterizing coal seam stress conditions and reflecting reservoir stress states through its composite attributes. This coefficient is a critical determinant affecting the permeability, fracturability, and gas production capacity of deep coal reservoirs. A larger horizontal principal stress difference tends to form single fractures, while a smaller difference facilitates complex fracture networks conducive to large-scale volumetric fracturing. The calculation formulas are as follows:

$$P_{sd} = \frac{SH_1 - SH_2}{SH_2} \quad (13)$$

Vertical stress is determined using density logging curves through a piecewise summation method. Maximum and minimum horizontal principal stresses are calculated using an anisotropic composite spring model.

$$\left\{ \begin{array}{l} \sigma_v = 0.00981 \times (\rho * TVD + \sum_{i=1}^n \rho_i * \Delta D_i) \\ SH_1 = \frac{PR}{1-PR} (\sigma_v - \alpha P_p) + \beta_1 \frac{E}{1+PR} (\sigma_v - \alpha P_p) + \alpha P_p \\ SH_2 = \frac{PR}{1-PR} (\sigma_v - \alpha P_p) + \beta_2 \frac{E}{1+PR} (\sigma_v - \alpha P_p) + \alpha P_p \end{array} \right. \quad (14)$$

where: σ_v is the vertical stress, MPa; TVD is the vertical depth of the formation without density logging, m; ρ is the average formation density in unlogged intervals (typically 2.31 g/cm³); ΔD_i is the vertical depth sampling interval, m; SH_1 is the maximum principal stresses, MPa; SH_2 is the minimum principal stresses, MPa; α is the effective stress coefficient, dimensionless; β_1 is Strains in maximum horizontal principal stress directions, mm; β_2 is Strains in minimum horizontal principal stress directions, mm; Other parameters maintain the same definitions as above.

(4) Fracturing pressure P_f

The rupture pressure is a key parameter for measuring whether a coal reservoir can be effectively fractured, which intuitively reflects the mechanical properties of the coal reservoir. Lower fracture pressure means that coal reservoirs are relatively easy to be fractured. Through techniques such as hydraulic fracturing, more fracture networks can be formed, thereby increasing the desorption and migration channels of coal rock gas and improving its production. Coal reservoirs with high fracture pressure also have relatively high mechanical strength, which has a certain impact on the stability of coal reservoirs and fracturing engineering construction. Based on the theory of maximum tensile stress, when the reservoir is composed of intact rock, the hydraulic pressure inside the well must overcome the tensile strength of the rock in order for tensile fractures to appear around the wellbore. At this point, the critical pressure of the formation is the fracture pressure, which is calculated using the following formula:

$$P_f = \frac{3SH_2 - SH_1 + S_t - \alpha \left(\frac{1-2PR}{1-PR} \right) P_p}{2 - \alpha \left(\frac{1-2PR}{1-PR} \right)} \quad (14)$$

where: P_f is the fracture pressure, MPa; S_t is the tensile strength of the coal seam, MPa; the meaning of other parameters is the same as above.

(5) Lateral pressure coefficient P_{lp}

The lateral pressure coefficient is defined as the ratio of mean horizontal principal stresses (maximum and minimum) to vertical principal stress, quantifying the relative magnitude between horizontal and vertical stresses in deep coal reservoirs. Values exceeding 1 suggest horizontal stress dominance, while values below 1 indicate vertical stress dominance. This coefficient positively correlates with formation permeability, where elevated values promote extended fracture propagation, consequently improving coal reservoir permeability and hydraulic fracturing performance. The calculation formula is:

$$P_{lp} = \frac{(SH_2 + SH_1)}{2\sigma_v} \quad (16)$$

where: P_{lp} is the coal seam lateral pressure coefficient, dimensionless; the meaning of other parameters is the same as above.

4 Principles and methods

4.1 Modeling principle and process of PSO-ELM algorithm

The Extreme Learning Machine (ELM) is a machine learning algorithm based on feedforward neural networks, proposed in 2004 by artificial intelligence expert Guang-Bin Huang (Yang Qi et al., 2024). As a single hidden layer learning system, it simplifies the parameter setting process and demonstrates advantages such as fast learning speed and strong generalization capability compared to other machine learning algorithms. It has been widely applied in data prediction for Earth sciences and related fields (Xie et al., 2024). The structural model of ELM is shown in figure 5.

Assuming there are n training samples (X_i, Y_i) , where the input $X_i = [x_{i1}, x_{i2}, \dots, x_{in}]^T$ and output $Y_i = [y_{i1}, y_{i2}, \dots, y_{im}]^T$, with l hidden layer nodes. Let $g(x)$ be the activation function, $\omega_i = [\omega_{i1}, \omega_{i2}, \dots, \omega_{im}]^T$ denotes the connection weights between the input and hidden layers, $\beta_i = [\beta_{i1}, \beta_{i2}, \dots, \beta_{im}]^T$ denote the hidden-output layer connection weights, and $b_i = [b_{i1}, b_{i2}, \dots, b_{il}]^T$ be the hidden layer biases. The ELM algorithm can be expressed as:

$$Y = H \times \beta \quad (17)$$

where H denotes the matrix of outputs from the hidden layer, articulated as:

$$H = \begin{bmatrix} g(\omega_1, b_1, x_1) & g(\omega_2, b_2, x_1) & \dots & g(\omega_l, b_l, x_1) \\ g(\omega_1, b_1, x_2) & g(\omega_2, b_2, x_2) & \dots & g(\omega_l, b_l, x_2) \\ \dots & \dots & \dots & \dots \\ g(\omega_1, b_1, x_n) & g(\omega_2, b_2, x_n) & \dots & g(\omega_l, b_l, x_n) \end{bmatrix}_{n \times l} \quad (18)$$

The equation system's least squares solution yields the connection weights between the hidden and output layers:

$$\min_{\beta} \|H\beta - T'\| = \|H\hat{\beta} - T'\| \quad (19)$$

Solving the above equation yields:

$$\hat{\beta} = H^+ T' \quad (20)$$

where: the Moore-Penrose generalized inverse of matrix H is denoted by H^+ , T' is the expected output matrix of samples, and T' is the transpose of matrix T .

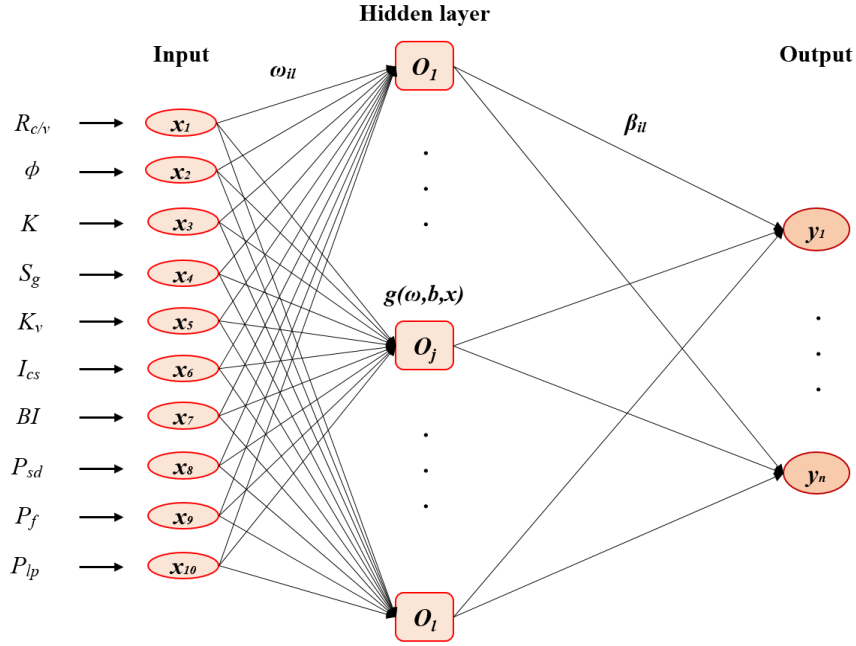


Figure 5. EML extreme learning machine structure diagram

Nonetheless, the connection weights of the input layer and hidden layer, as well as the biases of the hidden layer in the conventional ELM algorithm referenced above, are established arbitrarily (Hossam Faris et al, 2017). Although this method can simplify the process and improve computational speed, it cannot guarantee the reliability of the prediction results; relying solely on increasing the number of hidden layer nodes to improve prediction accuracy can lead to problems such as decreased model generalization ability (Li et al., 2024). Therefore, selecting the optimal model parameters before model training is the key to ensuring the accuracy of ELM prediction. The commonly used heuristic optimization method and grid search method for parameter optimization have a large computational load and high cost, which is not conducive to the efficient prediction of fracturing sweet spot interval intervals on site. This study decided to use Particle Swarm Optimization (PSO) algorithm for parameter optimization.

In ELM parameter optimization, PSO, a population-based optimization search technique, has demonstrated promising application outcomes. Figure 6 displays the PSO-ELM model's algorithm flow. There are five components to the workflow:

- (1) Initialize particle swarm, in n-dimensional space, use $x_i=(x_1, x_2, \dots, x_n)$ to represent the position vector of particles, use $v_i=(v_1, v_2, \dots, v_n)$ to represent the particle velocity vector;
- (2) Evaluate the fitness of particles;
- (3) Search for individual and overall optimal solutions;
- (4) Through iterative equations (21) and (22), update particle velocity and position;

$$v_i = \omega \times v_i + c_1 \times \alpha(p_i - x_i) + c_2 \times \beta(g_i - x_i) \quad (21)$$

$$x_i = x_i + v_i \quad (22)$$

where: ω is the inertia weight; c_1 and c_2 are learning factors, with a commonly used value of 2; α and β are the random number between (0,1); p_i is the individual optimal position, g_i is the global

optimal position.

The inertia weight ω significantly influences optimization results. An increased ω improves global search efficacy but diminishes local search, whereas a reduced ω yields the contrary effect (Han Y et al,2025). To better balance global and local search capabilities, this study adopts a dynamic ω strategy using a linearly decreasing weight formula:

$$\omega = \omega_{\max} - (\omega_{\max} - \omega_{\min}) \times \frac{k}{k_{\max}} \quad (23)$$

where: ω_{\max} denotes the upper bound of weight values; ω_{\min} denotes the lower bound of weight values; k denotes the number of iterations; k_{\max} denotes the maximum number of iterations.

(5) If the end condition is met, output the optimal weight and bias, otherwise switch to (2).

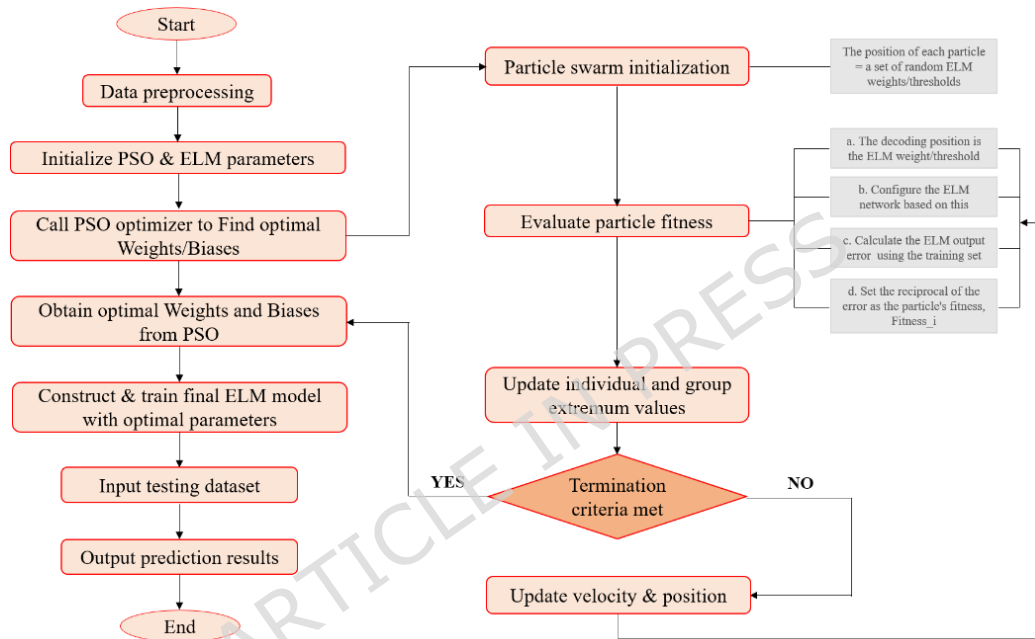


Figure 6. Flow chart of PSO-ELM algorithm

4.2 Constructing a classification evaluation model for fracturing sweet spot interval segments based on PSO-ELM algorithm

The construction of a grading evaluation model for deep coal reservoir fracturing sweet spot interval intervals is based on the PSO-ELM algorithm. The overall design idea is to first determine the sensitivity parameters closely related to geological engineering sweet spots, including reservoir quality and engineering quality evaluation parameters, and use them as several independent variables X_i ; Secondly, based on the actual fracturing effect analysis and production capacity data of the Research Area, the types of reservoir fracturing sweet spot interval intervals (Class I, II, III, IV) are determined, and the dataset is collected and organized as the Y value. At the same time, a quantitative standard table for reservoir fracturing sweet spot interval interval types is created, and the prediction results are expressed numerically in the specific application of the model; by adjusting the optimal combination of parameters to continuously optimize the model, the optimized model is finally applied to predict new data, to thoroughly evaluate the model's reliability.

(1) Dataset organization and standardization

The study selected 55 production wells, including X-5, X-1 to 1, X-8, X-10 to 4, which are widely distributed in the Research Area and have fracturing construction and production data. Initially, the aforementioned ten factors for reservoir quality and engineering quality evaluation are established as independent variables based on the analysis of logging interpretation data (Ma Y, 2020). Secondly, the fracturing effect of each single well is determined based on on-site experience and literature research. On the basis of comprehensive consideration of fracturing scale and post fracturing production capacity, it is quantified as the dependent variable. The Y value of this dependent variable corresponds to the classification criteria for reservoir fracturing sweet spot interval interval grading evaluation types: When $Y > 2.2$, the fracturing sweet spot interval interval is classified as Class I; when $1.8 < Y < 2.2$, the fracturing sweet spot interval interval is classified as Class II; when $1.4 < Y < 1.8$, the fracturing sweet spot interval interval is classified as Class III; When $Y < 1.4$, the fracturing sweet spot interval interval is classified as Class IV, and the prediction results are calibrated according to this standard.

From this, a dataset with 100 rows and 11 columns was organized, and the PSO-ELM algorithm was programmed on the Matlab platform. The dataset was then imported into the program for iterative prediction. To eliminate the influence of differences in the dimensionality and magnitude of different logging parameters on the prediction results, it is necessary to normalize the data of 10 independent variables and map the input curve values to $[0,1]$. According to the principles of well logging interpretation and rock mechanics theory, among the 10 independent variables, the carbon to plaster ratio R_{ρ} , porosity φ , permeability K , gas saturation S_g , coal texture I_{cs} , brittleness index BI , lateral pressure coefficient P_{lp} are positively correlated with the optimization target of sweet spots in reservoir fracturing; index of crack development degree K_v , horizontal stress difference coefficient P_{sd} , fracturing pressure P_f are negatively correlated with the optimal target for sweet spots in reservoir fracturing. Therefore, the above parameters are normalized in both forward and reverse directions.

$$\begin{cases} X^{+'} = \frac{X - X_{\min}}{X_{\max} - X_{\min}} \\ X^{-'} = \frac{X_{\max} - X}{X_{\max} - X_{\min}} \end{cases} \quad (24)$$

Where: $X^{+'}$ is the standardized positive parameter value, dimensionless; $X^{-'}$ is the standardized negative parameter value, dimensionless; X is the independent variable, with dimensions determined by the actual parameters; X_{\max} is the maximum independent variable value; X_{\min} is the minimum independent variable value.

(2) PSO-ELM algorithm modeling and accuracy analysis

Based on the PSO-ELM algorithm, a hierarchical evaluation model for fracturing sweet spot interval intervals in deep coal reservoirs was established using the aforementioned 100 sample datasets. The dataset was randomly split into training and testing sets at a 13:7 ratio, with the first

65 samples used for black-box model development and the remaining 35 samples for validation. Through actual training with 65 sets of data, it was found that the established black box model achieved an accuracy of 0.97, which is highly consistent with the true values (Figure 7a); in addition, the validation results of 35 sets of data show that the accuracy can still reach around 0.94 (Figure 7b), with a cumulative correct 31 layers and incorrect 4 layers, and a prediction accuracy rate of 88.57%. Finally, a regression relationship was established between the 100 predicted datasets and their corresponding true values (Figure 8). The results show a high degree of agreement between the data, with the model's overall prediction accuracy reaching approximately 0.94. This demonstrates that the hierarchical evaluation model for fracturing sweet spot interval interval intervals based on the PSO-ELM algorithm is scientifically robust and reliable, with broad prospects for practical application.

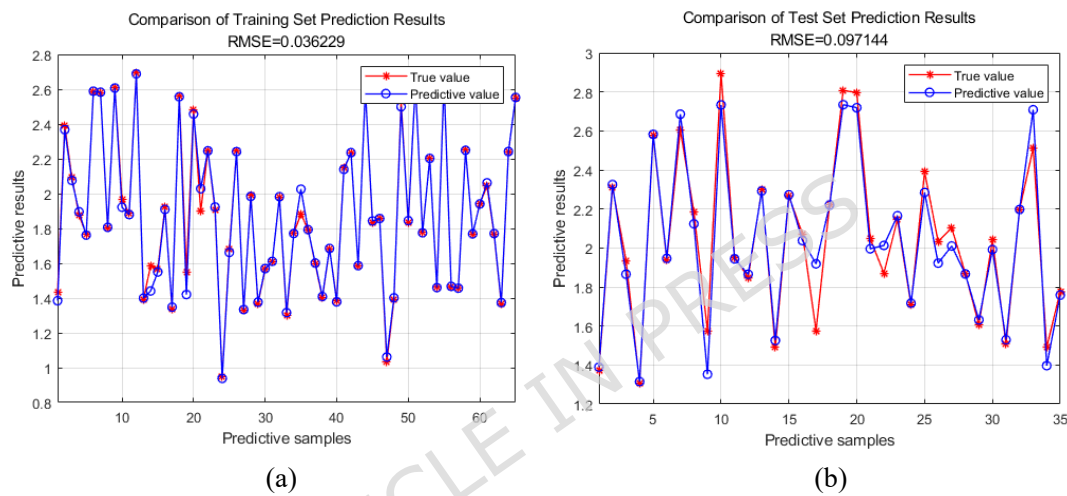


Figure 7. Modeling effect and accuracy verification results of PSO-ELM algorithm

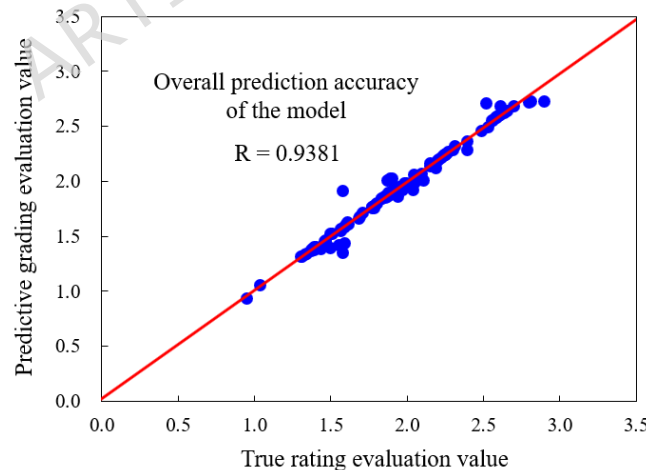


Figure 8. Overall accuracy analysis of PSO-ELM algorithm training and testing sets

5 Analysis and discussion

(1) Evaluation of actual well fracturing sweet spot interval interval section

Based on the PSO-ELM algorithm training mentioned above, a deep coal reservoir fracturing sweet spot interval interval segment grading evaluation model is developed. The black box model is saved in the Matlab platform program interface through the Save statement. X-11 well, which did

not participate in PSO-ELM algorithm training and testing, is selected for fracturing sweet spot interval interval segment prediction. The predicted results were compared with the actual fracturing sweet spot interval interval intervals to verify the model's accuracy.

As shown in figure 9, there are two main coal seams, No. 5 and No. 8, in the 2140-2210m depth section of X-11 well. The primary structural coal is developed, with a completeness degree of over 85%, mainly composed of semi dull coal (mirror coal and bright coal account for 40%). The black asphalt luster feature is obvious, showing a uniform structure, and two sets of cutting planes are developed roughly perpendicular to the bedding plane. The endogenous cutting planes have yellow filling and no exogenous cracks. The distribution depth of No. 5 coal is 2150.25-2153.875m, with a thickness of 3m after deducting the gangue layer; the distribution depth of No. 8 coal is 2194.625-2196.625m, with a thickness of 2m; in addition, two thin coal seams with a thickness of about 1m are developed at the top and bottom positions of No. 8 coal. According to on-site perforation and fracturing construction data, the actual Class I fracturing sweet spot interval interval section is 2150.25-2152.125m and 2194.625-2196.625m, with a total thickness of 3.875m; the actual Class II fracturing sweet spot interval interval section is 2152.75-2154.125m, with a thickness of 1.375m; the actual Class IV fracturing sweet spot interval interval section is 2152.125-2152.75m and 2190.75-2191.125m, with a total thickness of 1m.

By organizing the parameter data required for the PSO-ELM algorithm mentioned above, a total of 58 rows of data were collected. The black box model was used to predict and display the results, and four types of fracturing sweet spot interval intervals were predicted. The Class I fracturing sweet spot interval interval section is 2150.625-2152.25m and 2194.625-2196.25m, with a total of 33 predicted data lines. After comparison with actual working conditions, 27 lines of data were accurately predicted, and the other 6 lines of data were predicted as Class II fracturing sweet spot interval interval sections, including the upper part of No. 5 coal at 2150.25-2150.625m and the underpart of No. 8 coal at 2196.25-2196.625m, with a prediction accuracy of 81.8%; the second-class fracturing sweet spot interval interval section is 2152.75-2153.875m, with a total of 12 rows of predicted data. After comparison with the actual working conditions, 10 rows of data were predicted accurately, and the other 2 rows of data were predicted as the third class fracturing sweet spot interval interval section, which is 2153.875-2154.125m in the lower part of No. 8 coal seam, with a prediction accuracy of 83.3%; the IV type fracturing sweet spot interval interval section includes two thin coal seams, with a total of 10 predicted data lines. After comparison with actual working conditions, all 10 predicted data lines are accurate. As shown in figure 10, after comparing all predicted data with actual fracturing conditions, the overall prediction accuracy calculated exceeds 85%. This indicates that the PSO-ELM algorithm has good stability and prediction accuracy, and can be widely used.

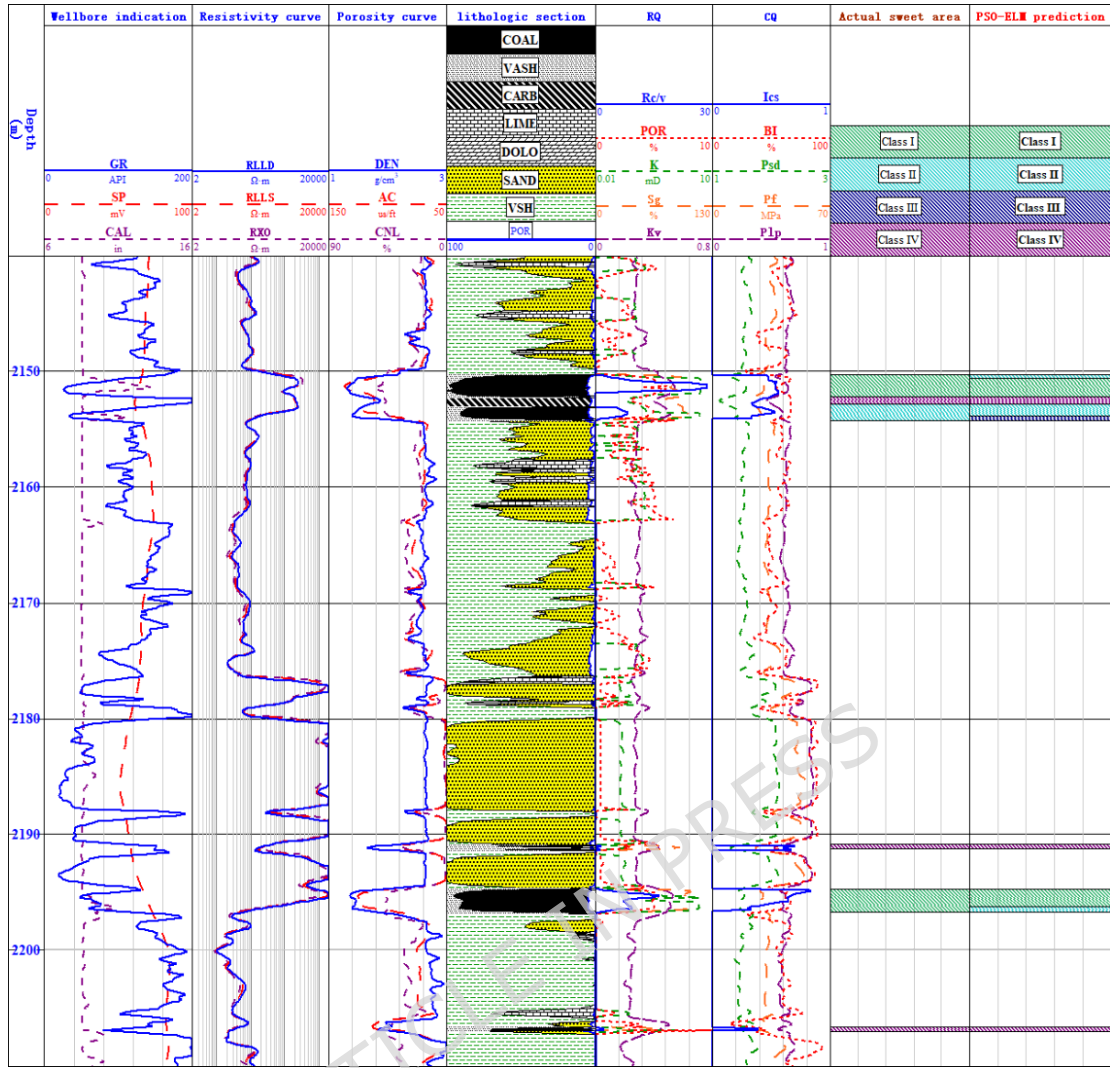


Figure 9. Results of fracturing sweet spot interval prediction by PSO-ELM algorithm for X-11 well in Research Area

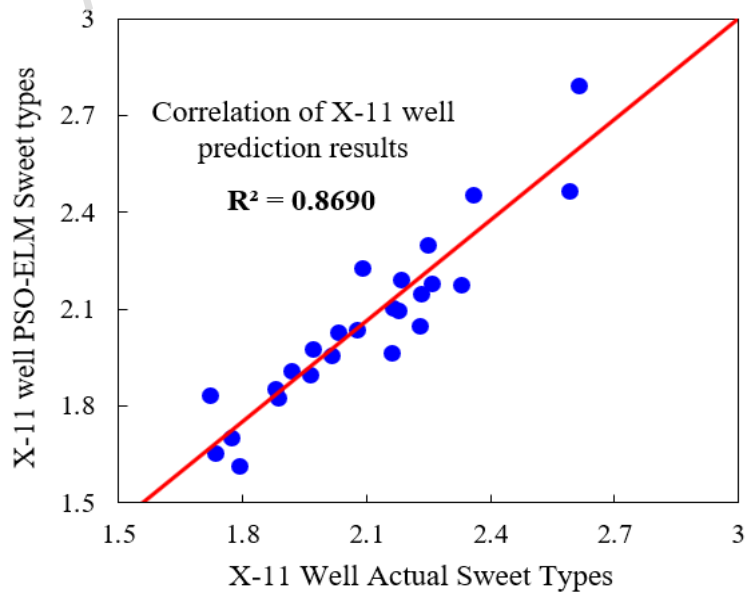


Figure 10. Accuracy analysis of PSO-ELM algorithm prediction results for X-11 well

(2) Research on the planar distribution characteristics of sweet spots in reservoir fracturing

Based on the above model, a detailed single-well interpretation and evaluation of deep coal reservoirs was conducted for dozens of wells in the Research Area. Building on this, a planar distribution study of fracturing sweet spot interval intervals in the reservoirs was carried out. Following the hierarchical evaluation criteria for reservoir fracturing sweet spot interval intervals (as shown in Figure 11), logging interpretation data were utilized to generate a hierarchical evaluation map of fracturing sweet spot interval intervals for the reservoirs in the Research Area on the Petrel platform.

From the map, it can be observed that:

- Class I fracturing sweet spot interval intervals are widely distributed across the Research Area but primarily concentrated in structural high positions in the central and southwestern regions. This is attributed to stable coal seam thickness distribution, favorable gas content, and permeability trends in these areas.
- Class II sweet spots are broadly distributed but generally clustered around Class I sweet spots, with no significant centralized distribution pattern. This indicates stable reservoir and engineering quality distributions, as well as a gradual transition between structural highs and lows.
- Class III sweet spots are mainly located in the central-southern and southeastern regions, covering smaller areas and predominantly surrounded by Class II sweet spots.
- Class IV sweet spots show no distinct distribution pattern across the block.

These observations demonstrate that high-quality sweet spots (Classes I – III) occupy a significant proportion of the Research Area's planar distribution, further confirming the substantial production potential of its deep coal reservoirs.

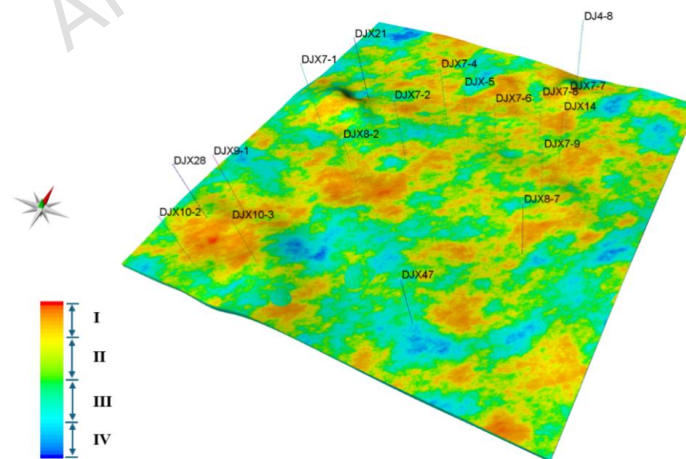


Figure 11. Distribution results of fracturing sweet points in coal reservoirs of Research Area

6 Conclusions

(1) The hierarchical evaluation model for reservoir fracturing sweet spot interval interval segments established based on the PSO-ELM algorithm can accurately predict the types of sweet spot segments in deep coal reservoirs within the Research Area. Its prediction results align with

actual fracturing conditions and gas testing outcomes, thereby validating the scientific rigor and reliability of the constructed model. This demonstrates its significant potential for broader application in deep coal seam development.

(2) The facturing sweet spot intervals of the deep coal reservoir in the Research Area is generally classified as Class I. The lithology of the top and bottom strata consists mainly of mudstone and some limestone, exhibiting poor fracability but favoring efficient coal seam fracturing. Spatially, the block is dominated by Class I and II sweet spot distributions, with numerous high-quality sweet spots identified as viable for development.

(3) The prediction of fracturing sweet spot interval intervals in deep coal rock gas reservoirs should be guided by the geology-engineering integration concept. Establishing a scientifically effective predictive model requires clarifying the dominant controlling factors influencing both geological and engineering quality in deep coal rock gas reservoirs, as well as elucidating how these factors contribute to fracturing effectiveness and productivity. This approach forms the foundation for developing an integrated predictive methodology system for fracturing sweet spot interval interval intervals identification in deep coal reservoirs.

Acknowledgements

This is a study on the evaluation of high-quality sweet spots in deep coal rock gas reservoirs. Dr. ZhiDi Liu expressed gratitude on behalf of all authors for the funding of the "Shaanxi Provincial Key R&D Program"; At the same time, we would like to express our gratitude to the Hancheng Gas Production Management Area and Linfen Gas Production Management Area of PetroChina Coal rock gas Co., Ltd. for their strong support in terms of data and technology; I also sincerely thank the Shaanxi Provincial Key Laboratory of Oil and Gas Reservoir Geology for providing experimental conditions support.

Funding

This work is supported by "Shaanxi Provincial Key R&D Program (No.2025CY-YBXM-163)".

Conflict of interest statement

The authors declare that they have no conflicts of interest.

Data availability statement

The training and testing data used in this article are all from PetroChina Coal rock gas Co., Ltd. As the data is under control, the unit has authorized Dr. Liu Zhi, the first corresponding author, to share the data through non-public channels only for academic exchange after the applicant has completed strict procedures.

Author Contributions

Dr. ZhiDi is responsible for the overall review and approval of the manuscript, providing key core ideas; Dr. Duo Wang, Binrui Yang and Jidong Tang are responsible for the complete writing

and review of the manuscript; Chengwang Wang, Wei Wang are responsible for providing and organizing necessary data, verifying completeness; Xinsi Hu, Jingnan Zhang are responsible for writing machine learning programs and drawing graphics; All authors have reviewed the manuscript.

References

- Tao Wang, Guoxiao Zhou, Liyong Fan *et al*, 2024. Full-Scale Pore and Microfracture Characterization of Deep Coal Reservoirs: A Case Study of the Benxi Formation Coal in the Daning–Jixian Block, China. *International Journal of Energy Research*, <https://doi.org/10.1155/2024/5772264>
- Lin J, 2019. Proceedings of the International Field Exploration and Development Conference 2019, Springer Series in Geomechanics and Geoengineering, <https://doi.org/10.1007/978-981-15-2485-1>
- Wang C, Zhen H, Chen G *et al*, 2022. Characteristics and Fracturability Evaluation of Deep No.8 Coal Reservoir in Daning-Jixian Block. *China Coal Geology*, **34**:1-5. <http://doi:10.3969/j.issn.1674-1803.2022.02.01>
- Wang C, Liu X, Li S *et al*, 2024. Analysis of the main controlling factors for deep coalbed methane enrichment in the Daning-Jixian block and evaluation of sweet spots in geological engineering. *Journal of Xi'an Petroleum University (Natural Science Edition)*, **39**:1-9. <http://doi:10.3969/j.issn.1673-064X.2024.04.001>
- Li S, Wang C, Wang H *et al*, 2022. Characteristics of Deep Coalbed methane Accumulation and Evaluation of Favorable Areas in Daning-Jixian Block. *Coalfield Geology and Exploration*, **50**: 59-67. <http://doi:10.12363/issn.1001-1986.21.12.0842>
- Allegra H S, Keyu L, Jianliang L *et al*, 2022. Chapter 18 - Integrating forward stratigraphic modeling with basin and petroleum system modeling, *Deepwater Sedimentary Systems Science, Discovery and Applications*, **11**: 625-672, <https://doi.org/10.1016/B978-0-323-91918-0.00002-5>
- Peng N, Zhang C, Feng R *et al*, 2024. Analysis of Dynamic Evolution of Surrounding Rock Movement and Stress-Fracture in the Upward and Repeated Mining of Close-Distance Coal Seams. *Advances in Civil Engineering*, **10**:1-17, <https://doi.org/10.1155/2024/5548837>
- Zheng G, Fan M, Guo D *et al*, 2024. Deep coalbed methane sweet spot characteristics and favorable area evaluation in Daning-Jixian District. *Journal of Xinjiang University (Natural Science Edition)*, **41**: 336-343. <http://doi:10.13568/j.cnki.651094.651316.2024.01.15.0002>
- Banerjee A, Chatterjee, R, 2021. A Methodology to Estimate Proximate and Gas Content Saturation with Lithological Classification in Coalbed methane Reservoir, Bokaro Field, India. *Natural Resources Research*, **30**:1-17. <http://doi:10.1007/s11053-021-09828-2>
- Liu J, Zhu G, Liu Y *et al*, 2023. Breakthrough and Future Challenges and Countermeasures in Deep Coalbed methane Exploration in the Eastern Margin of the Ordos Basin: A Case Study of the Linxing Shenfu Block. *Acta Petroleum Sinica*, **44**: 1827-1839. <http://doi:10.7623/syxb202311006>
- Xu F, Nie Z, Sun W *et al*, 2024. Theoretical and Technical System for Efficient Development of Deep Coalbed methane in the Eastern Margin of the Ordos Basin. *Journal of Coal Industry*, **49**: 528-544. <http://doi:10.13225/j.cnki.jccs.YH23.1290>
- Guo G, Xu F, Liu L *et al*, 2024. The Law of Deep Coalbed methane Accumulation and Evaluation of Favorable Areas in Fugu Area of Ordos Basin. *Coalfield Geology and Exploration*, **52**: 81-91. <http://doi:10.12363/issn.1001-1986.23.08.0521>
- Zhang H, 2013. A Research on Coal Reservoir Geological Modeling and its Application in Exploration and Development of the Coalbed methane. *Advanced Materials Research*, **734**:17-20. <http://doi:10.4028/www.scientific.net/AMR.734-737.17>
- Wang C, Liu Y, Guo G *et al*, 2016. Research on the prediction method of "sweet spot" coalbed methane in Shizhuang South Block. *Clean Coal Technology*, **22**:102-107. <http://doi:10.13226/j.issn.1006-6772.2016.03.022>
- Urosevic Milovan1 Brian J, 2000. The prediction of sweet-spots using 2-D seismic data. *AAPG Bulletin*, **84**. <http://doi:10.1306/a96750e8-1738-11d7-8645000102c1865d>
- Yan X, Xiong X, Li S *et al*, 2024. Contribution and main controlling factors of production in each section of deep coalbed methane horizontal wells: taking the Daning-Jixian block on the eastern edge of the Ordos Basin as an example. *Natural Gas Industry*, **44**:1-13. <http://doi:10.3787/j.issn.1000-0976.2024.10.006>
- Xu F, Nie Z, Sun W *et al*, 2024. Theoretical and Technical System for Efficient Development of Deep Coalbed

- methane in Daning-Jixian Block. *Journal of Coal Industry (in Chinese)*, **49**:1-17. <http://doi:10.13225/j.cnki.jccs.YH23.1290>
- Mondal D, Sang S, Han S *et al*, 2024. Coalbed methane reservoir properties assessment and 3D static modeling for sweet-spot prediction in Dahebian block, Liupanshui Coal field, Guizhou Province, southwestern China. *Heliyon*, **10**: 35481-35481. <http://doi:10.1016/j.heliyon.2024.e35481>
- Xia P, Zeng F, Song X, 2017. Geological structural controls on coalbed methane content of the No. 8 coal seam, Gujiao area, Shanxi, China. *Applied Ecology And Environmental Research*. **15**: 51-68. http://doi:10.15666/aecer/1501_051068
- Cheng Y, Liu Q, Ren T *et al*, 2021. Application of Coal Mechanics in Coal and Gas Outbursts. *Coal Mechanics*, 463–523, <https://doi.org/10.1007/978-981-16-3895-4>
- LIU Z, HAN H, WANG C *et al*. Calculation method of gas saturation and distribution characteristics of deep coal seam in Daning-Jixian block using logging data[J]. *Natural Gas Geoscience*, 2024, 35(2): 193-201. 10.11764/j.issn.1672-1926.2023.08.004
- V. Vishal, P.G. Ranjith, S.P. Pradhan *et al*, 2013. Permeability of sub-critical carbon dioxide in naturally fractured Indian bituminous coal at a range of down-hole stress conditions. *Engineering Geology*, **167**:148-156, <https://doi.org/10.1016/j.enggeo.2013.10.007>
- Tang S, Yang J, Tang D *et al*, 2023. Dynamic transformation law of gas occurrence state during deep coalbed methane reservoir formation process. The 7th Academic Symposium on Unconventional Oil and Gas Geological Evaluation, Abstract.
- Wei Y, Zhao L, Liu W *et al*, 2023. Coalbed methane Reservoir Parameter Prediction and Sweet-Spot Comprehensive Evaluation Based on 3D Seismic Exploration: A Case Study in Western Guizhou Province, China, *Energies*, **16**:351-367. <http://doi:10.3390/en16010367>
- Fu X, Meng Y, Li Z *et al*, 2021. Coalbed methane Potential Evaluation and Development Sweet Spot Prediction Based on the Analysis of Development Geological Conditions in Yangjiapo Block, Eastern Ordos Basin, China, *Geofluids*, **2021**:1-12. <http://doi:10.1155/2021/8728005>
- Dong Y, Wang J, Tian Z *et al*, 2018. Application of pseudo-linear Zoeppritz equation in the prediction of coalbed methane "sweet spot". *Society of Exploration Geophysicist*, **175271**:645-649. <http://doi:10.1190/segam2018-2992573.1>
- Wang D, Liu Z, 2024. Study and application of evaluation method for fracability of deep coalbed methane reservoir - taking the Daning-Jixian block in the Ordos Basin as an example. *International Journal of Oil, Gas and Coal Technology*, **35**: 407-441. <http://doi:10.1504/IJOGCT.2024.138685>
- Xun S, Zheng S, Wang J *et al*, 2023. Application of new rock mechanics stratigraphic methods in predicting the "sweet spot" of deep coalbed methane exploration and development. *Acta Petroleum Sinica (in Chinese)*, **44**:1840-1853. <http://doi:10.7623/syxb20231107>
- Li M, Cao Y, Ding R *et al*, 2024. Exploration of Gas Production Characteristics and Reserve Estimation Methods for Deep Coal and Rock Gas in Daning-Jixian Block. *China Petroleum Exploration*, **29**: 142-155. <http://doi:10.3969/j.issn.1672-7703.2024.04.011>
- Yang S, 2004. Geological Study of Coalbed methane in Daning-Jixian Area, Shanxi Province. *China University of Geosciences (Beijing)*.
- Yang Q, Chen J, Hua Z *et al*, 2024. Research on Life Prediction of PEMFC Based on Integrated Extreme Learning Machine, *Journal of Electrical Engineering (in Chinese)*, **40**:1-12. <http://doi:10.19595/j.cnki.1000-6753.tces.240123>
- Xie X, Luo B, Huang C *et al*, 2024. Underground Disease Identification Method Based on 3D Ground Penetrating Radar and PSO-ELM: A Case Study of Jinniu District, Chengdu City. *Surveying and Mapping Bulletin*, **8**: 54-59. <http://doi:10.13474/j.cnki.11-2246.2024.0810>
- Hossam Faris, Ibrahim Aljarah, Seyedali Mirjalili, 2017. Improved monarch butterfly optimization for unconstrained global search and neural network training. *Applied Intelligence*, **48**: 445–464, <https://doi.org/10.1007/s10489-017-0967-3>
- Han Y, Zeng F, Fu L, 2025. GA-PSO Algorithm for Microseismic Source Location. *Applied Sciences*, **15**:1841, <https://doi.org/10.3390/app15041841>
- Ma Y, 2020. Fuling Shale Gas Field. *Marine Oil and Gas Exploration in China*, 537-570, <https://doi.org/10.1007/978-3-662-61147-0>

Li B, Wang X, Di D *et al*, 2024. Prediction model of maximum stress for concrete pipes based on XGBoost-PSO algorithm. *Journal Structures*, **68**:7205-7209. [http:// doi:10.1016/J.ISTRUC.2024.107205](http://doi:10.1016/J.ISTRUC.2024.107205)

ARTICLE IN PRESS